

Finite-Size Effects on Kármán Vortex in Molecular Dynamics Simulation

Yuta Asano,^{1,*} Hiroshi Watanabe,^{1,2} and Hiroshi Noguchi¹

¹*Institute for Solid State Physics, The University of Tokyo, Kashiwa, Chiba 277-8581, Japan*

²*Department of Applied Physics and Physico-Informatics,
Keio University, Yokohama, Kanagawa 223-8522, Japan*

The characteristics of the Kármán vortex generated by a molecular dynamics (MD) simulation exhibit strong finite-size effects, and MD can only reproduce the experimental results qualitatively. Here, we seek the simulation conditions for quantitatively reproduce the vortex shedding frequency. We found that the finite-size effects are mainly caused by the interference of vortices and the nonuniformity of the fluid viscosity coefficient.

It is well known that an obstacle in a flow generates two rows of staggered vortices called Kármán vortex street behind the obstacle. Flows around an obstacle can be found in many places around us, such as airflow around a building, water flow around a screw propeller, and so forth. Because the Kármán vortex is a source of noise and vibration, it is crucially important to understand the flow characteristics around an obstacle in the engineering field. Especially, the flow around a circular cylinder is one of the most fundamental problems of fluid dynamics. Therefore, experimental and numerical studies have been conducted on the flow around the circular cylinder [1]. The shedding characteristics of the vortices are phenomenologically well understood for the Newtonian fluid. The shedding frequency is given experimentally by the following equation:

$$St = 0.212 - \frac{4.5}{Re}, \quad (1)$$

where $St = fD/V$ and $Re = \rho DV/\eta$ are the Strouhal number and Reynolds number, respectively (f : vortex shedding frequency, D : cylinder diameter, V : inflow velocity, ρ : fluid density, η : fluid viscosity coefficient).

The flow around the circular cylinder is also important in studying flow phenomena of complex fluids, such as the Toms effect [2] and the suppression of vortices [3] exhibited by polymer solutions, and cavitation in multiphase flow [4]. This is because the flow around the circular cylinder is the simplest model to study the interaction between the macroscopic flow and the microscopic behavior of the polymer and bubble nuclei. These complex fluids are extremely important in the engineering field because understanding the mechanism of the complex fluid is a key to improve transportation efficiency. However, the analysis of the complex fluid is challenging because molecular-scale dynamics and macroscale flow fields influence each other. Therefore, considering the microscopic behavior, mesoscale simulations have been developed such as the lattice Boltzmann method and the multi-particle collision dynamics. These methods are expected to allow us to discuss the complex fluids beyond the level of the Navier-Stokes equations that are commonly used in fluid dynamics. On the other hand, with the progress in computational power, a molecular dynamics (MD) simulation is conceivable as the most direct method. Flow phenomena that occur at relatively low

Reynolds numbers, such as Kármán vortex, can be generated by MD simulation [5–7]. Although MD simulation is advantageous to deal with phase transitions and polymer dynamics in the flow field directly, it suffers from strong finite-size effects.

To understand the finite-size effects on MD, we investigate the difference between the Strouhal number $St^{(MD)}$ obtained by MD simulation and the value predicted by Eq. (1). This relation Eq. (1) holds for not only macroscopic methods based on the Navier-Stokes equations but also mesoscale methods [8, 9]. However, the values obtained by the MD simulations are twice as large as the expected value [5–7]. Because both St and Re are dimensionless quantities that do not depend on a typical spatial scale such as the cylinder diameter, it is expected that the relation Eq. (1) also holds in MD simulation. Possible causes of the deviation are the influence of compressibility [10, 11] due to high flow velocity and the interference of vortices due to periodic boundary conditions [12, 13]. The effects can be investigated by changing the density for the compressibility and the channel width for the vortex interference. Therefore, in the present study, we investigate the condition that quantitatively reproduces Eq. (1) for the Kármán vortex behind the circular cylinder by the MD simulation.

We used the Weeks–Chandler–Andersen potential [14] $\phi = 4\epsilon[(\sigma/r)^{12} - (\sigma/r)^6 + 1/4]\theta(2^{\frac{1}{6}} - r)$ for the interparticle interaction of the fluid, where θ is the Heaviside function, r is interparticle distance, ϵ and σ represent the energy and the length scale, respectively. The mass of the particle is m . Hereafter, physical quantities are expressed in units of energy ϵ , length σ , and time $\tau_0 = \sigma\sqrt{m/\epsilon}$. The simulation box is almost the same as in Ref. [7] and is a rectangle with dimension $L_x \times L_y$, where $L_x = 3600$ and $500 \leq L_y \leq 5000$. The flow direction of the fluid is the x -direction. The periodic boundary condition is taken for both directions. The circular cylinder is modeled by a set of particles whose positions are fixed on the cylinder surface. The cylinder with diameter $D = 100$ is located at $(x, y) = (1000, L_y/2)$. To control the temperature and the inflow velocity, we used the Langevin thermostat [7] in the region of $3200 \leq x \leq 3600$. The friction coefficient of the Langevin thermostat (ζ of Eq. (4) in Ref. [7]) is 0.1 and is linearly increased from 0.0001 to 0.1 at $3200 \leq x \leq 3400$. The temperature is set to $T = 1$. This thermostat relaxes the velocities of the fluid particles into the Maxwell distribution whose average velocity is given by V in the x -direction. The density is in the range of $0.4 \leq \rho \leq 0.83$. In the three-dimensional (3D) simulations, the thickness of the simulation box in the

* yuta.asano@issp.u-tokyo.ac.jp

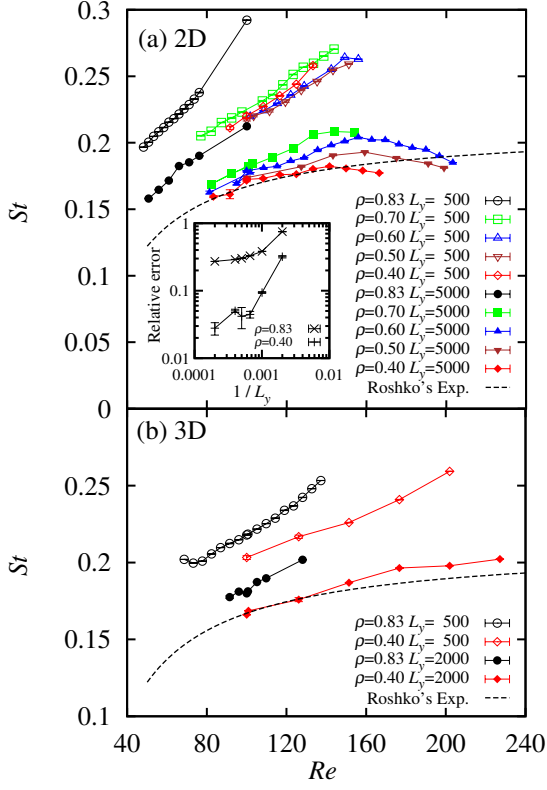


FIG. 1. (Color online) Strouhal number St as a function of the Reynolds number Re in (a) 2D and (b) 3D. The open and filled symbols show the results of the channel width $L_y=500$ and $L_y=5000$, respectively. The inset in panel (a) shows the relative error at $Re=100$ as a function of L_y .

z -direction $L_z = 10$ is employed. When Kármán vortices appear, a periodic lifting force F_L whose period is equal that of the vortex shedding acts on the cylinder. Here, we adopted the frequency of lift coefficient $C_L = 2F_L/(\rho DV^2)$ as the shedding frequency of the Kármán vortex. MD simulations were performed using the velocity-Verlet algorithm with a time step of 0.004, for up to a maximum of 10 000 000 time steps. The time integration is performed by LAMMPS [15].

Figure 1(a) shows the Re dependence of $St^{(MD)}$ in the two-dimensional (2D) simulations. The broken line in the figure shows Eq. (1). While all results deviate from Eq. (1) in the case of $L_y = 500$, the results of $L_y = 5000$ tend to approach Eq. (1). The inset of Fig. 1 shows the L_y dependence of the relative error of $\rho = 0.40, 0.83$ at $Re = 100$. The relative error is defined as $|St^{(MD)} - St|/St$. In the case of $\rho = 0.40$, the relative error decreases monotonically as L_y increases. Therefore, the interference of the vortex with the image cell is one of the main causes of the deviation from Eq. (1). As for $\rho = 0.83$, the relative error only reaches up to $\sim 30\%$ and the relative errors are almost unchanged between $L_y = 2500$ and $L_y = 5000$. This observation suggests that another cause also exists for this phenomenon at the high density. Figure 1(b) shows the results of the 3D simulations. Like the 2D simulations, $St^{(MD)}$ tends to approach Eq. (1) as L_y increases.

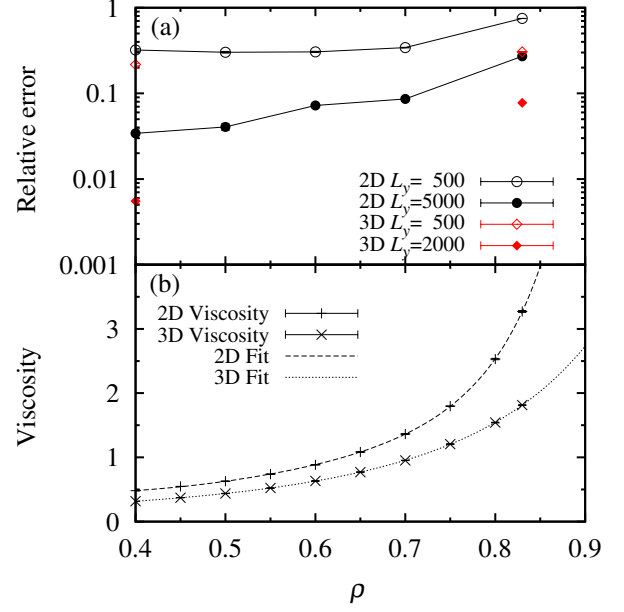


FIG. 2. (Color online) (a) Relative error at $Re = 100$ and (b) the viscosity as a function of the density. The open and filled symbols show the results of the channel width $L_y=500$ and $L_y=5000$, respectively. The dashed and dotted lines in (b) are obtained by fits using Eq. (19) in Ref. ([17]) with $d = 4$.

The density dependence of the relative error at $Re = 100$ is shown in Fig. 2(a). As the density decreases, the error at $L_y = 5000$ decreases monotonically while it is almost independent at $L_y = 500$ for the low density ($\rho \leq 0.6$). Therefore, the deviation from Eq. (1) decreases as the density decreases when the system is almost free from the interference of the vortices. As shown in Fig. 2(b), the viscosity increases rapidly with the density. Therefore, the variation in the viscosity due to the density change also increases with increasing the density. In the 2D case, typical density fluctuation of $\rho = 0.40$ and $\rho = 0.83$ at the cylinder wake are $\Delta\rho = 0.035$ and $\Delta\rho = 0.12$, respectively. Hence, we conclude that the nonuniformity of viscosity near the cylinder is the cause of St deviation at high density. The relative errors in 3D are smaller than those in 2D because the viscosity variation is smaller as shown in Fig. 2.

In summary, we evaluate the Strouhal number of a Kármán vortex behind a circular cylinder by MD simulations. The main causes of the deviation from the experimental results are the interference of vortices and the nonuniformity of the viscosity. The former can be suppressed by widening the channel width, and the latter can be reduced by decreasing density. Therefore, we conclude that a nanoscale Kármán vortex can be analyzed quantitatively by the MD simulation. It is also expected that the MD simulation is applicable to the analysis of complex fluids.

ACKNOWLEDGMENTS

This research was supported by MEXT as “Exploratory Challenge on Post-K computer (Challenge of Basic Science-

Exploring Extremes through Multi-Physics and Multi-Scale Simulations) and JSPS KAKENHI Grant No. JP15K05201. Computation was partially carried out by using the facilities of the Supercomputer Center, Institute for Solid State Physics, University of Tokyo.

-
- [1] C. H. K. Williamson, *Annu. Rev. Fluid Mech.* **28**, 477 (1996).
 - [2] G. E. Gadd, *Nature* **206**, 463 (1965).
 - [3] G. E. Gadd, *Nature* **211**, 169 (1966).
 - [4] A. Gnanaskandan, and K. Mahesh, *J. Fluid. Mech.* **790**, 453 (2016).
 - [5] R. C. Rapaport and E. Clementi, *Phys. Rev. Lett.* **57**, 695 (1986).
 - [6] D. C. Rapaport, *Phys. Rev. A* **36**, 3288 (1987).
 - [7] Y. Asano, H. Watanabe, and H. Noguchi, *J. Chem. Phys.* **148**, 144901 (2018).
 - [8] X. He and G. Doolen, *J. Comput. Phys.* **134**, 306 (1997).
 - [9] A. Lamura and G. Gompper, *Eur. Phys. J. E* **9**, 477 (2002).
 - [10] M. Sabanca and F. Durst, *Phys. Fluids* **15**, 1821 (2003).
 - [11] A. I. Osipov, A. V. Uvarov, and N. A. Vinnichenko, *Phys. Fluids* **18**, 105106 (2006).
 - [12] D. Sumner, S. S. T. Wong, S. J. Price, and M. P. Paidoussis, *J. Fluid. Struct.* **13**, 309 (1999).
 - [13] Z. Trávníček, A.-B. Wang, and W.-Y. Tu, *Exp. Fluids* **55**, 1679 (2014).
 - [14] J. D. Weeks, D. Chandler, and H. C. Andersen, *J. Chem. Phys.* **54**, 5237 (1971).
 - [15] S. J. Plimpton, *J. Comput. Phys.* **117**, 1 (1995).
 - [16] A. Roshko, NACA Report 1191 (1954), Printed in USA.
 - [17] R. Hartkamp, P. J. Daivis, and B. D. Todd, *Phys. Rev. E* **87**, 032155 (2013).